Journal of
Applied Crystallography
ISSN 0021-8898

Received 16 August 2006
Accepted 17 January 2007

X-ray reflectivity studies on the deoxyribonucleic acid adsorption by 3-β-[*N*-(*N*′,*N*′-dimethylaminoethane)carbamoyl]cholesterol monolayer with divalent ions

Tang-Lang Lin,[a]* Jui-Ching Wu,[a] U-Ser Jeng[b] and Hsin-Yi Lee[b]

[a]Department of Engineering and System Science, National Tsing Hua University, Hsinchu 300, Taiwan, and [b]National Synchrotron Radiation Research Center, Hsinchu 300, Taiwan. Correspondence e-mail: tllin@mx.nthu.edu.tw

The effect of adding divalent ions on the deoxyribonucleic acid (DNA) adsorption by a cationic lipid monolayer at the air–water interface was investigated by X-ray reflectivity on Langmuir–Blodgett films supported on silicon wafers. The films were prepared from a DC-Chol {3-β-[*N*-(*N*′,*N*′-dimethylaminoethane)carbamoyl]cholesterol} monolayer with 1 μM DNA in the subphase with different amounts of calcium ions added. It is found in this study that adding divalent ions, such as calcium ions, can enhance the DNA adsorption to interfaces. The adsorbed DNA layer thickness as determined by X-ray reflectivity is found to vary linearly with the square root of the ion concentration. This indicates that charge-screening effects and ion-mediated condensation play an important role in the DNA–cationic lipid monolayer interaction.

1. Introduction

The cationic lipid–DNA (deoxyribonucleic acid) liposome has been widely studied for gene delivery applications (Li & Ma, 2001). It is a nonviral method for gene therapy. Although many studies have made of the structure and interaction of cationic lipid–DNA complexes in bulk and in solution (Koltover *et al.*, 1998, 2000; McManus *et al.*, 2003; Wetzer *et al.*, 2001), there are few studies on their interactions at the air–water interface. Recently, there have been some studies on using the Langmuir–Blodgett (LB) technique to study the cationic lipid–DNA interaction at the air–water interface (Kago *et al.*, 1999; Okahata *et al.*, 1996; Chen, Wang, Shen *et al.*, 2002; Sastry *et al.*, 2000; Symietz *et al.*, 2004; McLoughlin *et al.*, 2005; Cárdenas *et al.*, 2005). The DNA molecules adsorbed onto supported cationic bilayers could form an aligned two-dimensional structure with regular spacing as revealed by atomic force microscopy studies (Fang & Yang, 1997). Furthermore, DNA adsorption on supported bilayers was shown to depend on the surface charge density (Clausen-Schaumann & Gaub, 1999). Kago *et al.* (1999) used *in-situ* X-ray reflectivity to study the adsorption of DNA by the cationic dimethyldioctadecylammonium lipid, $2C_{18}$-glu-$N^{+}2C_1$ at the air–water interface and found that the reflectivity profiles can only be fitted with a two-layer model, with a first layer of about 25 Å containing more DNA and a second layer of about 11 Å containing less DNA. They also found that when the complex was transferred onto the solid substrate, the thickness of the DNA layer as determined by reflectivity was found to be about 11 Å. Okahata *et al.* (1996) reported that when dipping from the cationic $2C_{18}$-glu-N^{+} /DNA monolayer, the DNA strands were aligned along the dipping direction with a spacing of 41 Å, as found by X-ray diffraction. The *in-situ* grazing-incident diffraction study of Symietz *et al.*(2004) showed that DNA adsorbed under a cationic lipid methyltrioctadecylammonium bromide (TODAB) monolayer at the air–water has an ordered structure with a DNA spacing from 40 to 32 Å as the surface pressure increased from 10 to 50 mN m^{-1}. Recently, there have also been Brewster angle microscopy studies on the interaction of DNA with lipid monolayers at the air–water interface (McLoughlin *et al.*, 2005; Cárdenas *et al.*, 2005). The complex of DNA and surfactant could form nano-patterns that may be useful for nanotechnology applications (Chen, Li & Liu, 2002; Dai *et al.*, 2005), such as making CdS nanoparticle/DNA LB films (Zhang *et al.*, 2002; Torimoto *et al.*, 1999).

Although the interaction of DNA with lipid bilayers has been well studied, there are still limited studies on the interaction of DNA with lipid monolayers at the air–water interface, especially on the effect of salts. The interaction of DNA with the bilayer is fundamentally different from the interaction with the monolayer. The DNA interaction with the monolayer is only on one side, the monolayer, and the other side (solution) is a free space. The DNA adsorbed on the monolayer is not completely confined in a two-dimensional space as in the bilayer. Recent studies of DNA condensation in two dimensions (in a bilayer) by divalent ions showed there is a critical ion concentration for the sharp transition from a loosely spaced DNA array to a more condensed state (Koltover *et al.*, 2000). Adding divalent ions would screen the negatively charged DNA and reduce the repulsion between the DNA confined between the lipid bilayers. Different ion species have their own critical condensation concentrations, which means ion size also matters. The effect of adding divalent ions on the DNA interaction with a cationic lipid monolayer has still not been studied much.

In our previous studies, it was found that one layer of DNA can be adsorbed on the cationic lipid DC-Chol {3-β-[*N*-(*N*′,*N*′-dimethylaminoethane)carbamoyl]cholesterol} monolayer at the air–water interface (Wu, Lin, Jeng, Lee & Gutberlet, 2006; Wu, Lin, Jeng & Torikai, 2006). In this study, LB films of DC-Chol/DNA prepared

using the LB technique at different calcium ion concentrations were studied by X-ray reflectivity.

2. Experimental

2.1. Materials

Linear DNA type XIV from herring testes was purchased from Sigma and used without further purification. The size of the DNA is between 400 and 1000 base pairs with a centre of distribution at 700 base pairs (Dias *et al.*, 2000). DC-Chol with a molecular weight of 537.3 Da was purchased from Sigma and used without further purification. The DNA solution was prepared at a concentration of 1 μM in H_2O and the solution was sonicated for 30 min for complete dissolution.

2.2. Langmuir–Blodgett films

Surface pressure–area isotherms were measured with a NIMA type 501 Langmuir–Blodgett trough. The temperature of the LB trough was kept at 293 $\pm$ 0.1 K by external water circulation. DNA solution at a concentration of 1 μM in H_2O was added with the desired amounts of $CaCl_2$. DC-Chol dissolved in chloroform was spread on the DNA solution. The isotherms were measured by compressing the barriers after waiting 30 min for chloroform evaporation. The barrier speed was set at 10 cm^2 min^{-1} and the trough area was 450 cm^2. The LB films for X-ray reflectivity measurements were transferred onto cleaned silicon wafers at a constant pressure and the transfer ratios for all samples were approximately 100%. The silicon wafers were immersed in the DNA solution all the time from the start of pouring the DNA solution into the LB trough.

2.3. X-ray reflectivity

The synchrotron X-ray reflectivity measurements were carried out at beamline 17A, a wiggler X-ray beamline at the National Synchrotron Radiation Research Center (NSRRC), Hsinchu, Taiwan. The wavelength of the incident X-rays was fixed at 1.334 Å. The software *Parratt32* (Hahn–Meitner Institute) was used in the X-ray reflectivity data analysis.

3. Results and discussions

3.1. Surface pressure–area isotherms

The surface pressure–area isotherms of pure DC-Chol and DC-Chol/DNA with different concentrations of $CaCl_2$ added are shown in Fig. 1. The presence of DNA in the subphase has significant effects on the isotherm. For the cases with DNA in the subphase, the surface pressure increases right from the beginning of compression. Without DNA in the subphase, the surface pressure does not rise at the beginning of compression. This is because the DC-Chol molecules dispersed at the surface interact with the DNA in the solution to form a condensed network at the air–water interface. For the cases with 1, 10, 50, 100 and 200 mM $CaCl_2$ added, the isotherms are similar but with slightly higher surface pressure rise with higher calcium ion concentrations at the beginning of compression. With higher calcium concentration, the repulsion between the DNA adsorbed by the DC-Chol at the surface is reduced and more DNA can be adsorbed by the surface to form more dense surface networks. The film collapse pressure also becomes lower for higher calcium concentrations, which means the film breaks earlier and could not tolerate higher compression. In the presence of calcium ions, at a compressed area of 50 $Å^2$, the surface pressure decreases initially with increasing calcium

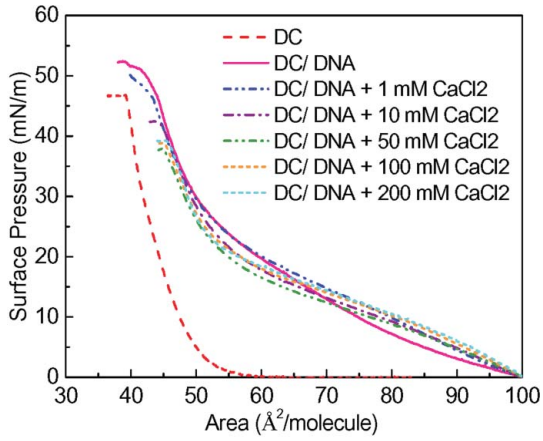

Figure 1
Surface pressure–area isotherms of pure DC-Chol and DC-Chol/DNA at different calcium ion concentrations.

ion concentration and reaches a minimum around 50 mM ion concentration. The surface pressure at a compressed area of 50 $Å^2$ gets higher as the ion concentration exceeds 50 mM. At higher ion concentrations, much more DNA molecules are adsorbed by the lipids at the air–liquid interface and the adsorbed DNA would also begin to exert a non-negligible surface pressure during the compression. This might be the reason why the surface pressure increases slightly at higher ion concentrations.

3.2. X-ray reflectivity

The LB films of DC-Chol/DNA with different amounts of $CaCl_2$ added were transferred onto cleaned silicon wafers. Fig. 2 shows the measured X-ray reflectivity of the LB films supported on silicon wafers together with the fitted curves. As shown in Fig. 2, clear fringes can be observed in the reflectivity curves, which means the DC-Chol/DNA films are very uniform. The reflectivity is shown as a function of

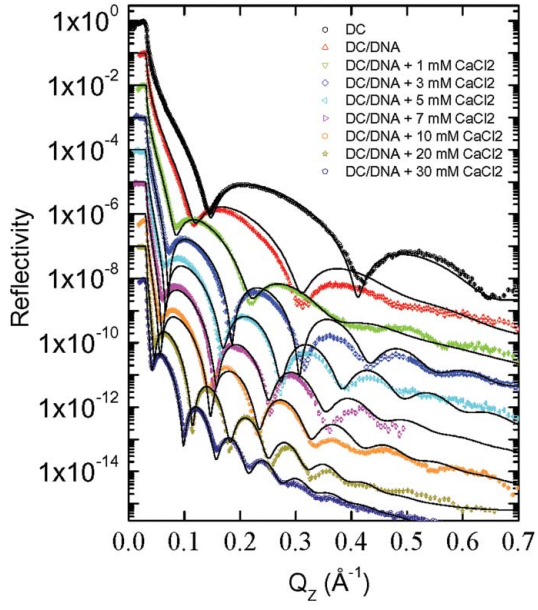

Figure 2
X-ray reflectivity profiles of the DC-Chol and DC-Chol/DNA LB films prepared at different calcium ion concentrations. Solid lines are the fitting results. The parameters determined from the fitting are listed in Table 1.

the vertical scattering vector Q_z. Here $Q_z = (4\pi/\lambda)\sin(\theta/2)$, where λ is the wavelength of the incident X-rays and θ is the scattering angle (the angle between the incident beam direction and the reflected beam direction). The size of the fringe decreases with increasing calcium concentration, which indicates an increase in film thickness with increasing calcium concentration. The results of the fits are listed in Table 1. In the fitting model, besides the lipid layer and DNA layer, an oxide layer of about 5 Å must also be taken into account. The surface roughness is found to increase from about 4 to 7 Å as the calcium ion concentration increased from 0 to 30 m*M*. It seems the surface becomes rougher when a thicker DNA layer is adsorbed. Adding more calcium ions will induce more DNA adsorption but there could also be more defects or irregularities. This is also shown by the interface roughness between the lipid and the DNA layer. This interfacial roughness increases from about 3 to 12 Å as the calcium concentration is increased from 0 to 30 m*M*. The reflectivity curves in Fig. 2 can be fitted quite well up to at least the second or the third fringe. For higher-order fringes, there are some deviations from the one DNA layer model used in this analysis. The slight deviations at higher-order fringes indicate slight scattering length density variations along the depth of the DNA layer. However, it would have very little effect on the accuracy of the layer thickness determined by the one DNA layer model used in this study. The uncertainty of the total film thickness determined from the fitting is quite small, since the fringe size is very sensitive to the total film thickness. For the thickness of each layer the uncertainty could be around 5%. The scattering length densities determined from the fitting could have uncertainties around 10%.

Fig. 3 shows the corresponding X-ray scattering length density (SLD) profiles as determined from the X-ray reflectivity data fitting results. Since the first adsorbed DNA layer could penetrate partially into the head group regions of the DC-Chol monolayer (Wu, Lin, Jeng, Lee & Gutberlet, 2006), there will not be a sharp interface between the DC-Chol and the DNA layer. The main part of the adsorbed DNA layer can be modelled as a uniform layer with a single SLD value. This could be due to the condensing effect when the film is prepared on a solid support even if it is not of uniform density at the air–water interface. Adding more calcium ions would increase the adsorbed DNA layer thickness with a similar SLD. The dependence of the adsorbed DNA layer thickness as a function of the square root of the added calcium ion concentration is plotted in Fig. 4. The DNA layer thickness is found to increase linearly with the square root of the calcium concentration. The first DNA array adsorbed to the DC-Chol is adsorbed through strong charge attraction between the negatively charged DNA and the ordered cationic DC-Chol monolayer. Additional DNA adsorption is through the DNA–DNA attraction mediated by the structured divalent calcium ions. The charge screening length constant is inversely proportional to the square root of the ion concentration in the solution. It is thus

Table 1
The fitting parameters for the X-ray reflectivity.

	Layer	Thickness (Å)	X-ray SLD ($\times 10^{-6}$ Å^{-2})	σ (Å)
DC	1 (Lipid)	19.1	9.2	3.5
	2 (SiO_2)	4.6	14.3	4
	Si	—	20.12	2
DC/DNA	1 (Lipid)	18	8.5	5
	2 (DNA)	8	11	3
	3 (SiO_2)	5	14.3	3
	Si	—	20.12	2
DC/DNA + 1 m*M* $CaCl_2$	1 (Lipid)	18	8.5	5.5
	2 (DNA)	20	10	6
	3 (SiO_2)	5	14.3	8
	Si	—	20.12	2
DC/DNA + 3 m*M* $CaCl_2$	1 (Lipid)	18	8	4
	2 (DNA)	28	10	5
	3 (SiO_2)	5	14.3	16
	Si	—	20.12	2
DC/DNA + 5 m*M* $CaCl_2$	1 (Lipid)	16	7.8	4
	2 (DNA)	36.3	10.5	8
	3 (SiO_2)	5	14.3	13
	Si	—	20.12	2
DC/DNA + 7 m*M* $CaCl_2$	1 (Lipid)	16	8	5
	2 (DNA)	41	10.5	6
	3 (SiO_2)	5	14.3	14
	Si	—	20.12	2
DC/DNA + 10 m*M* $CaCl_2$	1 (Lipid)	15	7.6	5
	2 (DNA)	47	10.5	8
	3 (SiO_2)	5	14.3	13
	Si	—	20.12	2
DC/DNA + 20 m*M* $CaCl_2$	1 (Lipid)	15	7.4	6.3
	2 (DNA)	68	11	10
	3 (SiO_2)	5	14.3	13
	Si	—	20.12	3
DC/DNA + 30 m*M* $CaCl_2$	1 (Lipid)	14	7	7
	2 (DNA)	84	11	12
	3 (SiO_2)	5	14.3	10
	Si	—	20.12	2

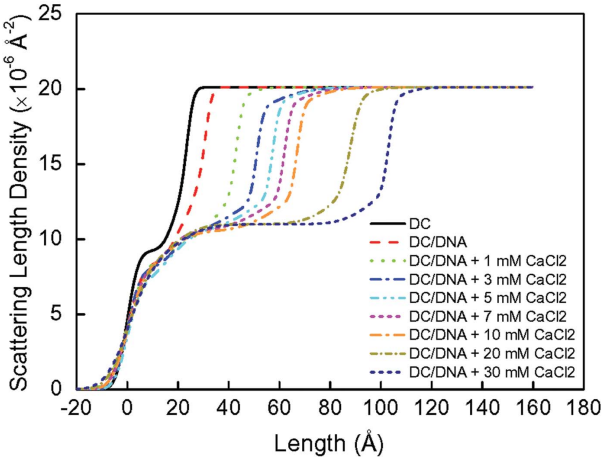

Figure 3
X-ray scattering length density profiles determined from fitting the reflectivity data.

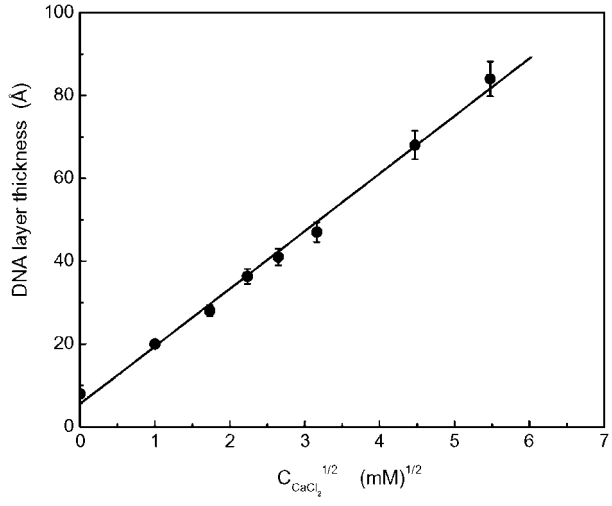

Figure 4
The adsorbed DNA layer thickness as a function of the square root of the calcium ion concentration. The error bars are the estimated 5% uncertainty in determining the layer thickness.

suspected that the linear growth of the adsorbed DNA layer with the square root of the ion concentration is related to the charge screening effect by the divalent ions. However, the condensation of DNA onto a two-dimensional surface is different from the DNA condensation in bulk. With the assistance of an ordered array of the first adsorbed DNA array, more stable second, third *etc.* DNA arrays can be adsorbed onto the surface with the help of calcium ions. Higher calcium concentrations are needed in order to condense a thicker DNA layer. Although part of the DNA in the DNA layer of the prepared DC-Chol/DNA film is deposited onto the silicon wafer when the silicon wafer is immersed in the DNA solution, it is still interesting to find that the condensation of DNA onto the surface monolayer and the silicon wafer are related to the charge screening effect in a linear way.

4. Conclusions

It is found in this study that adding divalent ions, such as calcium ions, can enhance the DNA adsorption to interfaces. The adsorbed DNA layer thickness as determined by X-ray reflectivity is found to vary linearly with the square root of the ion concentration. This indicates that charge screening effects and ion-mediated condensation play important roles in the DNA–cationic lipid monolayer interaction.

We would like to thank the NSRRC for the beam time and support during the measurements. This research is supported by the National Science Council, ROC, grant Nos. NSC 94-2113-M-007-003 and NSC95-2623-7-007-012-NU.

References

Cárdenas, M., Nylander, T., Jönsson, B. & Lindman, B. (2005). *J. Colloid Interface Sci.* **286**, 166–175.
Chen, X., Li, L. & Liu, M. (2002). *Langmuir*, **18**, 4449–4454.
Chen, X., Wang, J., Shen, N., Luo, Y., Li, L., Liu, M. & Thomas, R. K. (2002). *Langmuir*, **18**, 6222–6228.
Clausen-Schaumann, H. & Gaub, H. E. (1999). *Langmuir*, **15**, 8246–8251.
Dai, S., Zhang, X., Du, Z. & Dang, H. (2005). *Mater. Lett.* **59**, 423–429.
Dias, R., Mel'nikov, S., Lindman, B. & Miguel, M. G. (2000). *Langmuir*, **16**, 9577–9583.
Fang, Y. & Yang, J. (1997). *J. Phys. Chem. B*, **101**, 441–449.
Kago, K., Matsuoka, H., Yoshitome, R., Yamaoka, H., Ijiro, K. & Shimomura, M. (1999). *Langmuir*, **15**, 5193–5196.
Koltover, I., Salditt, T., Rädler, J. O. & Safinya, C. R. (1998). *Science*, **281**, 78–81.
Koltover, I., Wagner, K. & Safinya, C. R. (2000). *Proc. Natl Acad. Sci. USA*, **97**, 14046–14051.
Li, S. & Ma, Z. (2001). *Curr. Gene Ther.* **1**, 201–226.
McLoughlin, D., Dias, R., Lindman, B., Cardenas, M., Nylander, T., Dawson, K., Miguel, M. & Langevin, D. (2005). *Langmuir*, **21**, 1900–1907.
McManus, J. J., Rädler, J. O. & Dawson, K. A. (2003). *Langmuir*, **19**, 9630–9637.
Okahata, Y., Kobayashi, T. & Tanaka, K. (1996). *Langmuir*, **12**, 1326–1330.
Sastry, M., Ramakrishnan, V., Pattarkine, M., Gole, A. & Ganesh, K. N. (2000). *Langmuir*, **16**, 9142–9156.
Symietz, C., Schneider, M., Brezesinski, G. & Mölhwald, H. (2004). *Macromolecules*, **37**, 3865–3873.
Torimoto, T., Yamashita, M., Kuwabata, S., Sakata, T., Mori, H. & Yoneyama, H. (1999). *J. Phys. Chem. B*, **103**, 8779–8803.
Wetzer, B., Byk, G., Frederic, M., Airiau, M., Blanche, F., Pitard, B. & Scherman, D. (2001). *Biochem. J.* **356**, 747–756.
Wu, J. C., Lin, T. L., Jeng, U. S., Lee, H. Y. & Gutberlet, T. (2006). *Physica B*, **385–386**, 841–844.
Wu, J. C., Lin, T. L., Jeng, U. S. & Torikai, N. (2006). *Physica B*, **385–386**, 838–840.
Zhang, X., Jin, J., Wang, G., Yang, W. & Li, T. (2002). *Mater. Chem. Phys.* **77**, 899–902.